Available online at www.sciencedirect.com
SCIENCE DIRECT®
International Journal of Solids and Structures 42 (2005) 3261–3287
INTERNATIONAL JOURNAL OF SOLIDS and STRUCTURES
www.elsevier.com/locate/ijsolstr

A BEM solution to transverse shear loading of composite beams

V.G. Mokos, E.J. Sapountzakis *

Institute of Structural Analysis, School of Civil Engineering, National Technical University of Athens, Zografou Campus, GR-15773 Athens, Greece

Received 20 July 2004; received in revised form 4 November 2004
Available online 29 December 2004

Abstract

In this paper a boundary element method is developed for the solution of the general transverse shear loading problem of composite beams of arbitrary constant cross-section. The composite beam consists of materials in contact, each of which can surround a finite number of inclusions. The materials have different elasticity and shear moduli with same Poisson's ratio and are firmly bonded together. The analysis of the beam is accomplished with respect to a coordinate system that has its origin at the centroid of the cross-section, while its axes are not necessarily the principal ones. The transverse shear loading is applied at the shear centre of the cross-section, avoiding in this way the induction of a twisting moment. Two boundary value problems that take into account the effect of Poisson's ratio are formulated with respect to stress functions and solved employing a pure BEM approach, that is only boundary discretization is used. The evaluation of the transverse shear stresses is accomplished by direct differentiation of these stress functions, while both the coordinates of the shear center and the shear deformation coefficients are obtained from these functions using only boundary integration. Numerical examples with great practical interest are worked out to illustrate the efficiency, the accuracy and the range of applications of the developed method. The accuracy of the proposed shear deformation coefficients compared with those obtained from a 3-D FEM solution of the 'exact' elastic beam theory is remarkable.

Keywords: Transverse shear stresses; Shear center; Shear deformation coefficients; Composite; Beam; Effect of Poisson's ratio; Boundary element method

* Corresponding author. Tel.: +30 2107721718; fax: +30 2107721720.
E-mail addresses: vmoko@tee.gr (V.G. Mokos), cvsapoun@central.ntua.gr (E.J. Sapountzakis).

0020-7683/$ - see front matter © 2004 Elsevier Ltd. All rights reserved.
doi:10.1016/j.ijsolstr.2004.11.005

Nomenclature

A	area of composite cross-section
C	centroid of composite cross-section
E_j	modulus of elasticity of the jth material
G_j	shear modulus of the jth material
I_{yy}, I_{zz}, I_{yz}	moments of inertia with respect to y and z axes and the product of inertia of composite cross-section
K	number of materials
M	center of twist of composite cross-section
M_y, M_z	bending moments with respect to y and z axes
Q_y, Q_z	shear forces with respect to y and z axes
S	shear center of composite cross-section
y_S, z_S	coordinates of the shear center with respect to the centroid of cross-section
a_y, a_z, a_{yz}	shear deformation coefficients
Γ_j	boundary of the jth inclusion
κ_y, κ_z, κ_{yz}	shear correction factors
v	Poisson's ratio
$(\sigma_{xx})_j$	normal stress component in x direction
$(\tau_{xy})_j$, $(\tau_{xz})_j$	transverse (direct) shear stress components in y and z directions, respectively
$(\tau_\Omega)_j$	resultant transverse shear stress in the regions Ω_j
$(\tau_{xn})_j$, $(\tau_{xt})_j$	transverse shear stress components in directions $\boldsymbol{n}$ and $\boldsymbol{t}$, normal and tangential to the cross-section boundary Γ_j, respectively
$(\tau_\Gamma)_j$	resultant transverse shear stress to the cross-section boundary Γ_j
$(\Phi(y,z))_j$, $(\Theta(y,z))_j$	stress functions
Ω_j	region occupied by the jth material

1. Introduction

The problem of a homogeneous prismatic beam subjected in shear torsionless loading has been widely studied from both the analytical and numerical point of view. Both theoretical discussions concerning flexural shear stresses (Weber, 1924; Trefftz, 1935; Goodier, 1944), or the problem of the center of shear (Goodier, 1944; Osgood, 1943; Weinstein, 1947; Reissner and Tsai, 1972) and text books giving detailed representations of these topics (Timoshenko and Goodier, 1984; Sokolnikoff, 1956; Love, 1952) are mentioned among the extended analytical studies.

Numerical methods have also been used for the analysis of the aforementioned problem. Among these methods the majority of researchers have employed the finite element method based on assumptions for the displacement field (Mason and Herrmann, 1968) or introducing a stress function that fulfils the equilibrium equations for the evaluation of the shear stresses (Gruttmann et al., 1999, 1998; Koczyk, 1994) and the shear deformation coefficients (Gruttmann and Wagner, 2001). The boundary element method has also been employed by Sauer (1980) for the calculation of shear stresses based on Weber analysis (1924) and neglecting Poisson ratio v. BEM was also used for the calculation of the shear center location in an arbitrary homogeneous cross-section by Chou (1993) and for the presentation of a solution to the general flexure problem in an isotropic only simply connected arbitrary cross-section beam by Friedman and Kosmatka (2000). In this research effort the analysis is accomplished with respect only to the principal bending axes of the cross-section restricting in this way its generality.

Contrary to these many efforts, to the authors' knowledge very little work has been done on the corresponding problem of composite beams of arbitrary constant cross-section. In the pioneer work of Muskhelishvili (1963) the governing equations of the problem are formulated and an analytic solution of a composite cross-section of simple geometry is presented. Nouri and Gay (1994) presented a numerical solution for the shear problem of composite beams of simply connected materials in contact, of arbitrary cross-section, employing the 2-D FEM and taking into account the boundary conditions at the interfaces. In this reference the shear problem is formulated with respect to the principal bending axes system, which as it is stated below is different from the principal shear axes one, while the evaluation of the non-diagonal shear deformation coefficient is missing. Moreover, Fatmi and Zenzri (2004) based on the 'exact' elastic beam theory presented a numerical solution of the shear problem of composite beams of arbitrary cross-section employing the 3-D FEM. The last two references take into account the boundary conditions at the interfaces in contrast with all other research efforts in composite beams of arbitrary cross-section that ignore them (Pilkey, 2002), resulting in an analysis that is not completely rigorous. In the case of composite beams of thin-walled or laminated cross-sections the aforementioned problem can also be solved using the 'refined models' (Reddy, 1989; Touratier, 1992a,b; Karama et al., 2003). However, these models do not satisfy the continuity conditions of transverse shear stress at layer interfaces and assume that the transverse shear stress along the thickness coordinate remains constant, leading to the fact that kinematic or static assumptions cannot be always valid. It is also worth here noting that most of the commercial finite element packages can only handle the shear problem of homogeneous beams (MSC/NASTRAN, 1999), while the corresponding ones handling composite beams usually ignore the boundary conditions at the interfaces (SectionBuilder, 2002), with very few exceptions of scientific programs (Debard/RDM5.01, 1997). Finally, the BEM has not yet been used for the solution of the aforementioned problem.

In this paper a boundary element method is developed for the solution of the general transverse shear loading problem of composite beams of arbitrary constant cross-section. The composite beam consists of materials in contact, each of which can surround a finite number of inclusions. The materials have different elasticity and shear moduli with same Poisson's ratio and are firmly bonded together. The shear loading is applied at the shear center of the cross-section, avoiding in this way the induction of a twisting moment. The formulation of the problem follows the governing equations presented in Pilkey (2002). Two boundary value problems that take into account the effect of Poisson's ratio are formulated with respect to stress functions and solved employing a pure BEM approach, that is only boundary discretization is used. The evaluation of the transverse shear stresses at any interior point is accomplished by direct differentiation of these stress functions, while both the coordinates of the shear center and the shear deformation coefficients are obtained from these functions using only boundary integration. The essential features and novel aspects of the present formulation are summarized as follows.

(i) All basic equations are formulated with respect to an arbitrary coordinate system, which is not restricted to the principal axes.
(ii) The boundary conditions at the interfaces between different material regions have been considered.
(iii) There is no need of splitting the stress function into the sum of two alternate cross-section functions leading to resolved shear stresses. A stress function is introduced, which fulfils the equilibrium and compatibility equations and from which the transverse shear stresses at any interior point are obtained by direct differentiation.
(iv) The shear deformation coefficients are evaluated using an energy approach instead of Timoshenko's (Timoshenko and Goodier, 1984) and Cowper's (Cowper, 1966) definitions, for which several authors (Schramm et al., 1994; Schramm et al., 1997) have pointed out that one obtains unsatisfactory results or definitions given by other researchers (Stephen, 1980; Hutchinson, 2001), for which these factors take negative values.

(v) Finite element methods require the whole cross-section to be discretized into area elements and are also limited with respect to the shape (distortion) of the elements. BEM solutions require only boundary discretization resulting in line or parabolic elements instead of area elements of the FEM solutions, while a small number of line elements are required to achieve high accuracy.
(vi) The effect of the material's Poisson ratio v is taken into account.
(vii) The proposed method can be efficiently applied to homogeneous and composite beams of thin walled cross-section and to laminated composite beams, without the restrictions of the 'refined models'.

Numerical examples with great practical interest are worked out to illustrate the efficiency, the accuracy and the range of applications of the developed method. The accuracy of the proposed shear deformation coefficients compared with those obtained from a 3-D FEM solution of the 'exact' elastic beam theory (Fatmi and Zenzri, 2004) is remarkable.

2. Statement of the problem

Consider a prismatic beam of length L with an arbitrarily shaped composite cross-section consisting of materials in contact, each of which can surround a finite number of inclusions, with modulus of elasticity E_j, shear modulus G_j and common Poisson's ratio v, occupying the regions Ω_j ($j = 1, 2, \ldots, K$) of the y, z plane (Fig. 1). The materials of these regions are firmly bonded together and are assumed homogeneous, isotropic and linearly elastic. Let also the boundaries of the nonintersecting regions Ω_j be denoted by Γ_j ($j = 1, 2, \ldots, K$). These boundary curves are piecewise smooth, i.e. they may have a finite number of corners. Without loss of generality, it may be assumed that the beam end with centroid at point C is fixed, while the x-axis of the coordinate system is the line joining the centroids of the cross-sections.

When the beam is subjected to torsionless bending arising from a concentrated load Q applied at the shear center S of its free end composite cross-section, at a distance x from the fixed end, the internal forces are the shear forces Q_y, Q_z being the components of the concentrated load Q along y and z axes, respectively and the bending moments M_y, M_z given as

$$M_y = -Q_z(L - x) \quad M_z = Q_y(L - x) \tag{1a, b}$$

Taking into account that the beam is not subjected to external axial centroidal forces and following the assumption that plane sections normal to the axis of a line member before deformation remain plane after deformation, the normal component of stress acting on the beam composite cross-section is given as

$$(\sigma_{xx})_j = \frac{E_j}{E_1}\left[-\left(\frac{M_y I_{yz} + M_z I_{yy}}{\mathrm{I}_{yy} I_{zz} - I_{yz}^2}\right) y + \left(\frac{M_y I_{zz} + M_z I_{yz}}{I_{yy} I_{zz} - I_{yz}^2}\right) z\right] \tag{2}$$

where

$$I_{yy} = \sum_{j=1}^{K} \frac{E_j}{E_1} \int_{\Omega_j} z^2 \, \mathrm{d}\Omega_j \quad I_{zz} = \sum_{j=1}^{K} \frac{E_j}{E_1} \int_{\Omega_j} y^2 \, \mathrm{d}\Omega_j \quad I_{yz} = \sum_{j=1}^{K} \frac{E_j}{E_1} \int_{\Omega_j} yz \, \mathrm{d}\Omega_j \tag{3a, b, c}$$

are the moments of inertia with respect to y and z axes and the product of inertia of the composite cross-section, respectively. Substituting Eq. (1a,b) into Eq. (2) the normal component of stress can be written as

$$(\sigma_{xx})_j = \frac{E_j}{E_1}\left[\frac{L - x}{I_{yy} I_{zz} - I_{yz}^2}\left[Q_z\left(y I_{yz} - z I_{zz}\right) + Q_y\left(z I_{yz} - y I_{yy}\right)\right]\right] \tag{4}$$

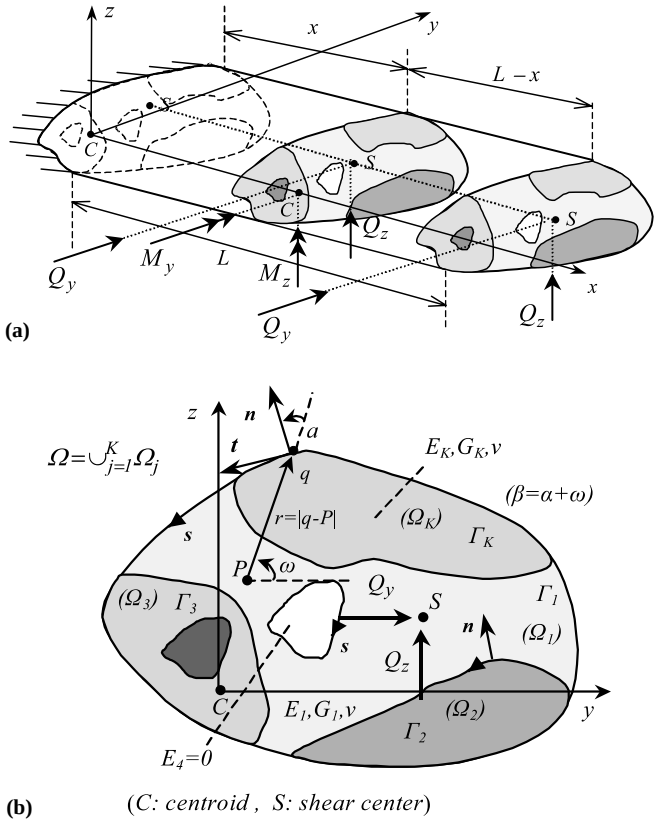

Fig. 1. Prismatic beam subjected to torsionless bending (a) and two dimensional region Ω occupied by the composite cross-section (b).

Following the Saint–Venant's assumption that the stress components $(\sigma_{yy})_j$, $(\sigma_{zz})_j$ and $(\tau_{yz})_j$ are negligibly small, the state of stress will be determined by evaluating the transverse (direct) shear stress components $(\tau_{xy})_j$ and $(\tau_{xz})_j$. Neglecting the body forces the last two equations of equilibrium of the three-dimensional elasticity can be written as

$$\frac{\partial(\tau_{xy})_j}{\partial x}=0 \quad \frac{\partial(\tau_{xz})_j}{\partial x}=0 \tag{5a, b}$$

leading to the conclusion that the shear stress distributions are functions of y and z, that is they are the same over any cross-section. The evaluation of these distributions will be accomplished by regarding the beam subjected separately to Q_y and Q_z shear forces and obtaining the arising shear stress components by superposition.

It is worth here noting that in the most general case of a composite cross-section with materials of different Poisson's ratios, the problem of torsionless bending becomes considerably more complicated, due to the fact that in this case the assumption of negligibly small stress components $(\sigma_{yy})_j$, $(\sigma_{zz})_j$ and $(\tau_{yz})_j$ is not correct (Muskhelishvili, 1963). However, having in mind that the values of the Poisson's ratios even for materials with significantly different elastic moduli are almost the same it follows that the aforementioned restriction is realistic.

Thus, considering the beam subjected only to Q_z shear force the first equation of equilibrium may be written as

$$\frac{\partial(\tau_{xy})_j}{\partial y}+\frac{\partial(\tau_{xz})_j}{\partial z}=\frac{E_j}{E_1}\frac{Q_z}{I_{yy}I_{zz}-I_{yz}^2}\left(yI_{yz}-zI_{zz}\right) \tag{6}$$

Using Hooke's stress–strain equations the resulting strain components satisfy identically four of the compatibility conditions. The rest two conditions using Eq. (4) for $Q_y=0$ can be written as

$$\frac{\partial}{\partial y}\left(\frac{\partial(\tau_{xz})_j}{\partial y}-\frac{\partial(\tau_{xy})_j}{\partial z}\right)=\frac{E_j}{E_1}\frac{vQ_zI_{zz}}{(1+v)\left(I_{yy}I_{zz}-I_{yz}^2\right)} \tag{7a}$$

$$\frac{\partial}{\partial z}\left(\frac{\partial(\tau_{xz})_j}{\partial y}-\frac{\partial(\tau_{xy})_j}{\partial z}\right)=\frac{E_j}{E_1}\frac{vQ_zI_{yz}}{(1+v)\left(I_{yy}I_{zz}-I_{yz}^2\right)} \tag{7b}$$

Assuming a stress function $(\Phi(y,z))_j$ having continuous partial derivatives up to the third order such that the two compatibility conditions (7a,b) to be identically satisfied, the transverse shear stress components $(\tau_{xy})_j$, $(\tau_{xz})_j$ and the resultant shear stress $(\tau_\Omega)_j$ in the regions Ω_j $(j=1,2,\ldots,K)$ are expressed as

$$(\tau_{xy})_j=E_j\frac{Q_z}{B}\left[\left(\frac{\partial\Phi}{\partial y}\right)_j-d_y\right] \tag{8a}$$

$$(\tau_{xz})_j=E_j\frac{Q_z}{B}\left[\left(\frac{\partial\Phi}{\partial z}\right)_j-d_z\right] \tag{8b}$$

$$(\tau_\Omega)_j=\left[(\tau_{xy})_j^2+(\tau_{xz})_j^2\right]^{1/2} \tag{8c}$$

where d_y, d_z are the y, z components of the vector $\boldsymbol{d}$ defined by

$$\boldsymbol{d}=d_y\boldsymbol{i}_y+d_z\boldsymbol{i}_z=\left[v\left(I_{zz}yz-I_{yz}\frac{y^2-z^2}{2}\right)\right]\boldsymbol{i}_y+\left[-v\left(I_{zz}\frac{y^2-z^2}{2}+I_{yz}yz\right)\right]\boldsymbol{i}_z \tag{9}$$

in which $\boldsymbol{i}_y$,$\boldsymbol{i}_z$ denote the unit vectors along the y and z axes and B is defined as

$$B=E_1\Delta=E_1 2(1+v)\left(I_{yy}I_{zz}-I_{yz}^2\right) \tag{10}$$

depending on the moduli of elasticity, the Poisson's ratio and the cross-section geometry. Substituting Eqs. (8a,b) in Eq. (6), the partial Poisson type differential equation governing the stress function $(\Phi(y,z))_j$ is obtained as

$$\left(\nabla^2\Phi\right)_j=2\left(I_{yz}y-I_{zz}z\right)\quad\text{in }\Omega_j\ (j=1,2,\ldots,K) \tag{11}$$

where $(\nabla^2)_j\equiv(\partial^2/\partial y^2)_j+(\partial^2/\partial z^2)_j$ is the Laplace operator and $\Omega=\bigcup_{j=1}^{K}\Omega_j$ denotes the whole region of the composite cross-section.

The boundary conditions of the aforementioned stress function will be derived from the following physical considerations:

- The traction vector in the direction of the normal vector $\boldsymbol{n}$ vanishes on the free surface of the beam, that is

$$(\tau_{xn})_j=(\tau_{xy})_j n_y+(\tau_{xz})_j n_z=0 \tag{12a}$$

- The traction vectors in the direction of the normal vector $\boldsymbol{n}$ on the interfaces separating the j and i different materials are equal in magnitude and opposite in direction, that is

$$(\tau_{xn})_j = (\tau_{xn})_i \quad \text{or} \quad (\tau_{xy})_j n_y + (\tau_{xz})_j n_z = (\tau_{xy})_i n_y + (\tau_{xz})_i n_z \tag{12b}$$

- The displacement components remain continuous across the interfaces, since it is assumed that the materials are firmly bonded together

where $n_y = \cos\beta$, $n_z = \sin\beta$ are the direction cosines of the normal vector $\boldsymbol{n}$ to the boundaries Γ_j $(j = 1, 2, \ldots, K)$, with $\beta = \widehat{y, \boldsymbol{n}}$ (see Fig. 1). It is worth noting that on both sides of the equality of (12b) the normal vector $\boldsymbol{n}$ points in one and the same direction, while the third physical consideration ensures the continuity of the stress function $(\Phi(y,z))_j$ inside the region Ω_j $(j = 1, 2, \ldots, K)$ as well as across the boundaries separating different materials $((\Phi)_j = (\Phi)_i)$.

Substituting Eqs. (8a,b) in Eqs. (12a,b), the Neumann type boundary condition of the stress function can be written as

$$E_j \left(\frac{\partial \Phi}{\partial n}\right)_j - E_i \left(\frac{\partial \Phi}{\partial n}\right)_i = (E_j - E_i)\boldsymbol{n} \cdot \boldsymbol{d} \quad \text{on } \Gamma_j \ (j = 1, 2, \ldots, K) \tag{13}$$

where E_i is the modulus of elasticity of the Ω_i region at the common part of the boundaries of Ω_j and Ω_i regions, or $E_i = 0$ at the free part of the boundary of Ω_j region, while $(\partial/\partial n)_j \equiv n_y(\partial/\partial y)_j + n_z(\partial/\partial z)_j$ denotes the directional derivative normal to the boundary Γ_j. The vector $\boldsymbol{n}$ normal to the boundary Γ_j is positive if it points to the exterior of the Ω_j region. It is worth here noting that the normal derivatives across the interior boundaries vary discontinuously.

Similarly, considering the beam subjected only to Q_y shear force and assuming the stress function $(\Theta(y,z))_j$ having continuous partial derivatives up to the third order such that all the compatibility conditions to be identically satisfied, the transverse shear stress components τ_{xy}, τ_{xz} are expressed as

$$(\tau_{xy})_j = E_j \frac{Q_y}{B}\left[\left(\frac{\partial \Theta}{\partial y}\right)_j - e_y\right] \tag{14a}$$

$$(\tau_{xz})_j = E_j \frac{Q_y}{B}\left[\left(\frac{\partial \Theta}{\partial z}\right)_j - e_z\right] \tag{14b}$$

where e_y, e_z are the y, z components of the vector e defined by

$$\boldsymbol{e} = e_y \boldsymbol{i}_y + e_z \boldsymbol{i}_z = \left[\nu\left(I_{yy}\frac{y^2 - z^2}{2} - I_{yz} yz\right)\right]\boldsymbol{i}_y + \left[\nu\left(I_{yy} yz + I_{yz}\frac{y^2 - z^2}{2}\right)\right]\boldsymbol{i}_z \tag{15}$$

Substituting Eqs. (14a,b) in the first equation of equilibrium of the three-dimensional elasticity and in the boundary condition (12a,b) the following Neumann problem for the stress function $(\Theta(y,z))_j$ is obtained as

$$(\nabla^2 \Theta)_j = 2(I_{yz} z - I_{yy} y) \quad \text{in } \Omega_j \ (j = 1, 2, \ldots, K) \tag{16}$$

$$E_j \left(\frac{\partial \Theta}{\partial n}\right)_j - E_i \left(\frac{\partial \Theta}{\partial n}\right)_i = (E_j - E_i)\boldsymbol{n} \cdot \boldsymbol{e} \quad \text{on } \Gamma_j \ (j = 1, 2, \ldots, K) \tag{17}$$

Having in mind that the shear center S is defined as the point of the cross-section at which the torsional moment arising from the transverse shear stresses vanishes, the coordinates $\{y_S, z_S\}$ of this point with respect to the system of axes with origin the cross-section centroid can be derived from the condition

$$y_S Q_z - z_S Q_y = M_x \Rightarrow y_S Q_z - z_S Q_y = \sum_{j=1}^{K} \int_{\Omega_j} \left[(\tau_{xz})_j y - (\tau_{xy})_j z \right] \mathrm{d}\Omega_j \tag{18}$$

For $Q_y = 0$, after substituting Eqs. (8a,b) in Eq. (18), the y_S coordinate of the shear center S can be obtained from

$$y_S = \frac{1}{B} \sum_{j=1}^{K} \int_{\Omega_j} E_j \left[y \left(\frac{\partial \Phi}{\partial z} \right)_j - z \left(\frac{\partial \Phi}{\partial y} \right)_j - y d_z + z d_y \right] \mathrm{d}\Omega_j \tag{19}$$

Similarly, for $Q_z = 0$ after substituting Eqs. (14a,b) in Eq. (18), the z_S coordinate of the shear center S can be obtained from

$$z_S = \frac{1}{B} \sum_{j=1}^{K} \int_{\Omega_j} E_j \left[z \left(\frac{\partial \Theta}{\partial y} \right)_j - y \left(\frac{\partial \Theta}{\partial z} \right)_j - z e_y + y e_z \right] \mathrm{d}\Omega_j \tag{20}$$

Eqs. (19) and (20) denote that the $\{y_S, z_S\}$ coordinates of the shear center S are independent from shear loading. Moreover, it can be shown that in the case of zero Poisson's ratio, the coordinates of the shear center S and the center of twist M coincide, that is

$$y_S = y_M \quad z_S = z_M \tag{21a, c}$$

where the equations for the coordinates $\{y_M, z_M\}$ are given in Sapountzakis (2000). This coincidence of these centers was first recognized by Weber (1924) by applying the Betty–Maxwell reciprocal relations.

Furthermore, the shear deformation coefficients a_y, a_z and $a_{yz} = a_{zy}$ which are introduced from the approximate formula for the evaluation of the shear strain energy per unit length (Schramm et al., 1997)

$$U_{\text{appr.}} = \frac{a_y Q_y^2}{2AG_1} + \frac{a_z Q_z^2}{2AG_1} + \frac{a_{yz} Q_y Q_z}{2AG_1} \tag{22}$$

are evaluated equating this approximate energy with the exact one given from

$$U_{\text{exact}} = \sum_{j=1}^{K} \frac{E_1}{E_j} \int_{\Omega_j} \frac{(\tau_{xz})_j^2 + (\tau_{xy})_j^2}{2G_1} \mathrm{d}\Omega_j \tag{23}$$

and are obtained for the cases $\{Q_y \neq 0, Q_z = 0\}$, $\{Q_y = 0, Q_z \neq 0\}$ and $\{Q_y \neq 0, Q_z \neq 0\}$, respectively, as

$$a_y = \frac{1}{\kappa_y} = \frac{A}{E_1 \Delta^2} \sum_{j=1}^{K} \int_{\Omega_j} E_j \left((\nabla \Theta)_j - \boldsymbol{e} \right) \cdot \left((\nabla \Theta)_j - \boldsymbol{e} \right) \mathrm{d}\Omega_j \tag{24a}$$

$$a_z = \frac{1}{\kappa_z} = \frac{A}{E_1 \Delta^2} \sum_{j=1}^{K} \int_{\Omega_j} E_j \left((\nabla \Phi)_j - \boldsymbol{d} \right) \cdot \left((\nabla \Phi)_j - \boldsymbol{d} \right) \mathrm{d}\Omega_j \tag{24b}$$

$$a_{yz} = \frac{1}{\kappa_{yz}} = \frac{A}{E_1 \Delta^2} \sum_{j=1}^{K} \int_{\Omega_j} E_j \left((\nabla \Phi)_j - \boldsymbol{d} \right) \cdot \left((\nabla \Theta)_j - \boldsymbol{e} \right) \mathrm{d}\Omega_j \tag{24c}$$

where

$$A = \sum_{j=1}^{K} \frac{G_j}{G_1} \int_{\Omega_j} \mathrm{d}\Omega_j \tag{25}$$

is the area of the composite cross-section, Δ is defined from Eq. (10), while $(\nabla)_j \equiv \boldsymbol{i}_y(\partial/\partial y)_j + \boldsymbol{i}_z(\partial/\partial z)_j$ is a symbolic vector. Employing the shear deformation coefficients a_y, a_z, a_{yz} using Eqs. (24a,b,c) we can define the cross-section shear rigidities of the Timoshenko's beam theory as

$$G_1 A_{sy} = G_1 A/a_y \tag{26a}$$

$$G_1 A_{sz} = G_1 A/a_z \tag{26b}$$

$$G_1 A_{syz} = G_1 A/a_{yz} \tag{26c}$$

In the case of an asymmetric cross-section the principal shear axes, defined as (Schramm et al., 1997)

$$\tan 2\varphi^S = \frac{2a_{yz}}{a_y - a_z} \tag{27}$$

do not coincide with the principal bending ones, defined by the engineering beam theory. Due to this difference, the deflection components in the y and z directions are in general coupled, even if the system of axes of the cross-section coincides with the principal bending one (Pilkey, 2002). If the cross-section is symmetric about an axis, the principal shear axes system coincides with the principal bending one. In this case, the deflection components with respect to the principal directions are not coupled any more ($a_{yz} = a_{zy} = 0$ and $I_{yz} = I_{zy} = 0$).

It is worth here noting that the reduction of Eqs. (2) and (3a,b,c) using the modulus of elasticity E_1 and of Eqs. (22), (23), (25) and (26a,b,c) using the shear modulus G_1 of the first material, could be achieved using any other material, considering it as reference material.

Finally, considering the beam subjected only to Q_z shear force the shear stress components at points on the boundary Γ_j ($j = 1, 2, \ldots, K$) are evaluated from the established values of $(\Phi)_j$ and $(\partial\Phi/\partial n)_j$ using the following relations

$$(\tau_{xn})_j = E_j \frac{Q_z}{B}\left[\left(\frac{\partial \Phi}{\partial n}\right)_j - \boldsymbol{n}\cdot\boldsymbol{d}\right] \tag{28a}$$

$$(\tau_{xt})_j = E_j \frac{Q_z}{B}\left[\left(\frac{\partial \Phi}{\partial t}\right)_j + d_y \sin\beta - d_z \cos\beta\right] \tag{28b}$$

$$(\tau_\Gamma)_j = \left[(\tau_{xn})_j^2 + (\tau_{xt})_j^2\right]^{1/2} \tag{28c}$$

where the tangential derivative $(\partial\Phi/\partial t)_j = (\partial\Phi/\partial s)_j$ is computed numerically using appropriately central, backward or forward differences. It is worth noting that $(\tau_{xn})_j$ is the bond stress at the interface part of the boundary Γ_j, while $(\tau_\Gamma)_j$ is the resultant boundary shear stress.

Similarly, considering the beam subjected only to Q_y shear force the shear stress components at points on the boundary Γ_j ($j = 1, 2, \ldots, K$) are evaluated from the established values of $(\Theta)_j$ and $(\partial\Theta/\partial n)_j$ as

$$(\tau_{xn})_j = E_j \frac{Q_y}{B}\left[\left(\frac{\partial \Theta}{\partial n}\right)_j - \boldsymbol{n}\cdot\boldsymbol{e}\right] \tag{29a}$$

$$(\tau_{xt})_j = E_j \frac{Q_y}{B}\left[\left(\frac{\partial \Theta}{\partial t}\right)_j + e_y \sin\beta - e_z \cos\beta\right] \tag{29b}$$

3. Integral representations—numerical solution

According to the precedent analysis, the shear problem of a composite beam reduces in establishing the stress functions $(\Phi(y,z))_j$ and $(\Theta(y,z))_j$ having continuous partial derivatives up to the third order, satisfying the governing equations (11) and (16) inside the regions Ω_j $(j=1,2,\ldots,K)$ of the y, z plane and the boundary conditions (13) and (17) on the corresponding boundary Γ_j, respectively.

The numerical solution of the boundary value problems described by Eqs. (11), (13) and (16), (17) is similar. For this reason, in the following we will analyze the solution of the problem of Eqs. (11) and (13) noting any alteration or addition for the problem of Eqs. (13) and (17).

The evaluation of the stress function $(\Phi(y,z))_j$ is accomplished using BEM as this is presented in Sapountzakis (2000). According to this method, the Green identity

$$\int_{\Omega_j}\left(\Psi\left(\nabla^2\Phi\right)_j-(\Phi)_j\nabla^2\Psi\right)\mathrm{d}\Omega_j=\int_{\Gamma_j}\left(\Psi\left(\frac{\partial\Phi}{\partial n}\right)_j-(\Phi)_j\frac{\partial\Psi}{\partial n}\right)\mathrm{d}s \tag{30}$$

when applied to the stress function $(\Phi)_j$ and to the fundamental solution

$$\Psi=\frac{1}{2\pi}\ln r(P,Q)\quad P,Q\in\Omega_j \tag{31}$$

which is a particular singular solution of the equation

$$\nabla^2\Psi=\delta(P,Q) \tag{32}$$

yields

$$\varepsilon(\Phi(P))_j=\int_{\Omega_j}\ln r\left(\nabla^2\Phi(Q)\right)_j\mathrm{d}\Omega_Q+\int_{\Gamma_j}\left((\Phi(q))_j\frac{\cos a}{r}-\left(\frac{\partial\Phi(q)}{\partial n}\right)_j\ln r\right)\mathrm{d}s_q \tag{33}$$

with $\alpha=\widehat{r,\boldsymbol{n}}$; $r=|P-q|$, $P,Q\in\Omega_j$, $q\in\Gamma_j$ $(j=1,2,\ldots,K)$ and $\varepsilon=2\pi$, π or 0 depending on whether the point P is inside the region Ω_j, $P\equiv p$ on the boundary Γ_j or P outside Ω_j, respectively. Note that the boundary has been assumed to be smooth at the point $p\in\Gamma_j$. Using Eq. (11) the integral representation (33) is written as

$$\varepsilon(\Phi(P))_j=\int_{\Omega_j}f(Q)\ln r\,\mathrm{d}\Omega_Q+\int_{\Gamma_j}\left((\Phi(q))_j\frac{\cos a}{r}-\left(\frac{\partial\Phi(q)}{\partial n}\right)_j\ln r\right)\mathrm{d}s_q \tag{34}$$

where the function f is defined as

$$f=2\left(I_{yz}y-I_{zz}z\right) \tag{35}$$

Applying once more the Green identity given by (30) for the function f satisfying the following equation

$$\nabla^2 f=0 \tag{36}$$

and for the function U defined as

$$U=\frac{1}{8\pi}r^2(\ln r-1) \tag{37}$$

satisfying the following equation

$$\nabla^2 U=\Psi \tag{38}$$

the domain integral of Eq. (34) can be converted into a line integral along the boundaries of the cross-section and the integral representation (34) is written as

$$\varepsilon(\Phi(P))_j = \frac{1}{4}\int_{\Gamma_j}\left(f(q)(2\ln r-1)r\cos a - \frac{\partial f(q)}{\partial n}(\ln r-1)r^2\right)\mathrm{d}s_q + \int_{\Gamma_j}\left((\Phi(q))_j\frac{\cos a}{r} - \left(\frac{\partial\Phi(q)}{\partial n}\right)_j\ln r\right)\mathrm{d}s_q \tag{39}$$

In Eq. (39) the subscript q in the arc element $\mathrm{d}s_q$ indicates that point q varies along the boundaries of the cross-section during integration and differentiation, while the point P (or p) is retained constant. The values of the function $(\Phi(P))_j$ inside the region Ω_j can be established from the integral representation (39) if $(\Phi)_j$ and its derivative $(\partial\Phi/\partial n)_j$ were known on the boundaries Γ_j. Thus,

$$(\Phi(P))_j = \frac{1}{8\pi}\int_{\Gamma_j}\left(f(q)(2\ln r-1)r\cos a - \frac{\partial f(q)}{\partial n}(\ln r-1)r^2\right)\mathrm{d}s_q + \frac{1}{2\pi}\int_{\Gamma_j}\left((\Phi(q))_j\frac{\cos a}{r} - \left(\frac{\partial\Phi(q)}{\partial n}\right)_j\ln r\right)\mathrm{d}s_q,\quad P\in\Omega_j,\ \ q\in\Gamma_j \tag{40}$$

The unknown boundary quantities $(\Phi)_j$ and $(\partial\Phi/\partial n)_j$ can be evaluated from the solution of a boundary integral equation on the boundary Γ_j, which is derived working as follows.

We consider a point p lying on the boundary Γ_j ($j=1,2,\ldots,K$). For a point q lying on the boundary Γ_j of the region Ω_j Eq. (39) may be written as

$$\pi(\Phi(p))_j = \frac{1}{4}\int_{\Gamma_j}\left(f(q)(2\ln r-1)r\cos a - \frac{\partial f(q)}{\partial n}(\ln r-1)r^2\right)\mathrm{d}s_q + \int_{\Gamma_j}\left((\Phi(q))_j\frac{\cos a}{r} - \left(\frac{\partial\Phi(q)}{\partial n}\right)_j\ln r\right)\mathrm{d}s_q,\quad q\in\Gamma_j \tag{41}$$

Similarly, for a point q lying on the part of the boundary Γ_k of the region Ω_k, which is an interface between regions Ω_j and Ω_k, Eq. (39) may be written as

$$\pi(\Phi(p))_j = \frac{1}{4}\int_{\Gamma_k}\left(-f(q)(2\ln r-1)r\cos a + \frac{\partial f(q)}{\partial n}(\ln r-1)r^2\right)\mathrm{d}s_q + \int_{\Gamma_k}\left(-(\Phi(q))_k\frac{\cos a}{r} + \left(\frac{\partial\Phi(q)}{\partial n}\right)_k\ln r\right)\mathrm{d}s_q,\quad q\in\Gamma_k \tag{42}$$

Moreover, for a point q lying on the boundaries Γ_i ($i=1,2,\ldots,K, i\neq k$) Eq. (39) yields

$$0 = \frac{1}{4}\int_{\Gamma_i}\left(-f(q)(2\ln r-1)r\cos a + \frac{\partial f(q)}{\partial n}(\ln r-1)r^2\right)\mathrm{d}s_q + \int_{\Gamma_i}\left(-(\Phi(q))_i\frac{\cos a}{r} + \left(\frac{\partial\Phi(q)}{\partial n}\right)_i\ln r\right)\mathrm{d}s_q,\quad q\in\Gamma_i \tag{43}$$

Notice that the sign in Eqs. (42) and (43) is reversed, since the unit vector normal to the boundary is negative.

Multiplying Eq. (41) by E_j, Eq. (42) by E_k, Eq. (43) by E_i ($i=1,2,\ldots,K, i\neq k$) and adding them yields

$$\pi(\Phi(p))_j(E_j+E_k) = \frac{1}{4}\sum_{j=1}^{K}\int_{\Gamma_j}(E_j-E_i)\left(f(q)(2\ln r-1)r\cos a - \frac{\partial f(q)}{\partial n}(\ln r-1)r^2\right)\mathrm{d}s_q + \sum_{j=1}^{K}\int_{\Gamma_j}\left[(E_j-E_i)(\Phi(q))_j\frac{\cos a}{r} - \left[E_i\left(\frac{\partial\Phi(q)}{\partial n}\right)_j - E_j\left(\frac{\partial\Phi(q)}{\partial n}\right)_i\right]\ln r\right]\mathrm{d}s_q \tag{44}$$

Using Eq. (13) and substituting Eq. (34) in Eq. (44), the following singular boundary integral equation is obtained

$$\begin{aligned}\pi(\Phi(p))_j\left(E_j+E_k\right)&=\frac{1}{2}\sum_{j=1}^{K}\int_{\Gamma_j}\left(E_j-E_i\right)\left[\left(I_{yz}y-I_{zz}z\right)(2\ln r-1)r\cos a-\left(I_{yz}\cos\beta-I_{zz}\sin\beta\right)(\ln r-1)r^2\right]\mathrm{d}s_q\\&+\sum_{j=1}^{K}\int_{\Gamma_j}\left(E_j-E_i\right)\left[(\Phi(q))_j\frac{\cos a}{r}-(\boldsymbol{n}\cdot\boldsymbol{d})\ln r\right]\mathrm{d}s_q\end{aligned}\tag{45}$$

It is worth here noting that in Eq. (45) the point p lies on the boundary Γ_j ($j=1,2,\ldots,K$), which is an interface between regions Ω_j and Ω_k, while the point q varies along the boundary Γ_j ($j=1,2,\ldots,K$), which is an interface between regions Ω_j and Ω_i, while $E_k=E_i=0$ in the case Γ_j is a free boundary. Moreover, in Eq. (45) the normal $\boldsymbol{n}$ to the boundary Γ_j points to the exterior of the region Ω_j and Γ_j is traveled only once.

For any given geometry of the composite cross-section the stress function $(\Phi(s))_j$ on the boundary Γ_j ($j=1,2,\ldots,K$) is obtained from the solution of the boundary integral equation (45). Thus, using constant boundary elements to approximate the line integrals along the boundaries and a collocation technique the following linear system of simultaneous algebraic equations is established

$$[A]\{\Phi\}=\{C\}\tag{46}$$

where

$$\{\Phi\}^{\mathrm{T}}=\left\{\left((\Phi)_1\right)_1\quad\left((\Phi)_1\right)_2\quad\cdots\quad\left((\Phi)_1\right)_M\quad\left((\Phi)_2\right)_{M+1}\quad\cdots\quad\left((\Phi)_K\right)_N\right\}\tag{47}$$

are the values of the boundary quantities $(\Phi)_j$ at the nodal points of the N boundary elements. Moreover, in Eq. (46) $[A]$ and $\{C\}$ are square $N\times N$ and column $N\times 1$ known coefficient matrices, respectively. From the solution of the system of simultaneous algebraic equations (46) the values of the stress function $(\Phi)_j$ for all boundary nodal points are established. Notice that the stress function $(\Phi)_j$ is determined exactly apart from an arbitrary constant term (Neumann problem). However, the stress components, the coordinates of the shear center and the shear deformation coefficients are not influenced by this arbitrary constant, since according to Eqs. (8a,b), (19), (20) and (24a,b,c) only the derivatives of $(\Phi)_j$ are required for the evaluation of these quantities.

The derivatives of $(\Phi)_j$ with respect to y and z at any interior point of the region Ω_j, for the calculation of the stress resultants (Eqs. (8a,b)) are computed differentiating the integral representation (Eq. 40) of the stress function $(\Phi)_j$ as

$$\begin{aligned}\left(\frac{\partial\Phi(P)}{\partial y}\right)_j&=\frac{1}{2\pi}\int_{\Gamma_j}\left((\Phi(q))_j\frac{\cos(\omega-a)}{r^2}+\left(\frac{\partial\Phi(q)}{\partial n}\right)_j\frac{\cos\omega}{r}\right)\mathrm{d}s_q\\&+\frac{1}{4\pi}\int_{\Gamma_j}\left(\left(I_{zz}z-I_{yz}y\right)(2\cos\omega\cos a+(2\ln r-1)\cos\beta)\right.\\&\left.-\left(I_{zz}\sin\beta-I_{yz}\cos\beta\right)(2\ln r-1)r\cos\omega\right)\mathrm{d}s_q\end{aligned}\tag{48a}$$

$$\begin{aligned}\left(\frac{\partial\Phi(P)}{\partial z}\right)_j&=\frac{1}{2\pi}\int_{\Gamma_j}\left((\Phi(q))_j\frac{\sin(\omega-a)}{r^2}+\left(\frac{\partial\Phi(q)}{\partial n}\right)_j\frac{\sin\omega}{r}\right)\mathrm{d}s_q\\&+\frac{1}{4\pi}\int_{\Gamma_j}\left(\left(I_{zz}z-I_{yz}y\right)(2\sin\omega\cos a+(2\ln r-1)\sin\beta)\right.\\&\left.-\left(I_{zz}\sin\beta-I_{yz}\cos\beta\right)(2\ln r-1)r\sin\omega\right)\mathrm{d}s_q\end{aligned}\tag{48b}$$

with $r=|P-q|$, $P\in\Omega_j$, $q\in\Gamma_j$ and $\omega=\widehat{x,r}$.

The derivative $(\partial\Phi/\partial n)_j$ for the evaluation of the shear stresses is known only on the free parts of the boundaries Γ_j. Its values on the interfaces can be established from Eq. (13) and the solution of the singular integral equation (41) using the boundary values of $(\Phi)_j$ obtained from the solution of Eq. (45).

Similarly, for any given geometry of the composite cross-section the stress function $(\Theta(s))_j$ on the boundaries Γ_j $(j = 1,2,\ldots,K)$ is obtained from the solution of the following singular boundary integral equation

$$\begin{aligned}
&\pi(\Theta(p))_j(E_j + E_k)\\
&= \frac{1}{2}\sum_{j=1}^{K}\int_{\Gamma_j}(E_j - E_i)\left[(I_{yz}z - I_{yy}y)(2\ln r - 1)r\cos a - (I_{yz}\sin\beta - I_{yy}cos\beta)(\ln r - 1)r^2\right]\mathrm{d}s_q\\
&\quad + \sum_{j=1}^{K}\int_{\Gamma_j}(E_j - E_i)\left[(\Theta(q))_j\frac{\cos a}{r} - (\boldsymbol{n}\cdot\boldsymbol{e})\ln r\right]\mathrm{d}s_q
\end{aligned} \tag{49}$$

while the values of the derivative $(\partial\Theta/\partial n)_j$ can be established from Eq. (17) and the solution of the following singular boundary integral equation

$$\begin{aligned}
\pi(\Theta(p))_j &= \int_{\Gamma_j}\left((\Theta(q))_j\frac{\cos a}{r} - \left(\frac{\partial\Theta(q)}{\partial n}\right)_j\ln r\right)\mathrm{d}s_q\\
&\quad + \frac{1}{2}\int_{\Gamma_j}\left((I_{yz}z - I_{yy}y)(2\ln r - 1)r\cos a - (I_{yz}\sin\beta - I_{yy}\cos\beta)(\ln r - 1)r^2\right)\mathrm{d}s_q
\end{aligned} \tag{50}$$

using the boundary values of $(\Theta)_j$ obtained from the solution of Eq. (49). Moreover, the values of the function $(\Theta(P))_j$ at any interior point of the region Ω_j can be established from the following integral representation as

$$\begin{aligned}
(\Theta(P))_j &= \frac{1}{2\pi}\int_{\Gamma_j}\left((\Theta(q))_j\frac{\cos a}{r} - \left(\frac{\partial\Theta(q)}{\partial n}\right)_j\ln r\right)\mathrm{d}s_q\\
&\quad + \frac{1}{4\pi}\int_{\Gamma_j}\left((I_{yz}z - I_{yy}y)(2\ln r - 1)r\cos a - (I_{yz}\sin\beta - I_{yy}\cos\beta)(\ln r - 1)r^2\right)\mathrm{d}s_q
\end{aligned} \tag{51}$$

while, the derivatives of $(\Theta)_j$ with respect to y and z axis from the following integral representations

$$\begin{aligned}
\left(\frac{\partial\Theta(P)}{\partial y}\right)_j &= \frac{1}{2\pi}\int_{\Gamma_j}\left((\Theta(q))_j\frac{\cos(\omega - a)}{r^2} + \left(\frac{\partial\Theta(q)}{\partial n}\right)_j\frac{\cos\omega}{r}\right)\mathrm{d}s_q\\
&\quad + \frac{1}{4\pi}\int_{\Gamma_j}\left((I_{yy}y - I_{yz}z)(2\cos\omega\cos a + (2\ln r - 1)\cos\beta)\right.\\
&\quad \left. - (I_{yy}\cos\beta - I_{yz}\sin\beta)(2\ln r - 1)r\cos\omega\right)\mathrm{d}s_q
\end{aligned} \tag{52a}$$

$$\begin{aligned}
\left(\frac{\partial\Theta(P)}{\partial z}\right)_j &= \frac{1}{2\pi}\int_{\Gamma_j}\left((\Theta(q))_j\frac{\sin(\omega - a)}{r^2} + \left(\frac{\partial\Theta(q)}{\partial n}\right)_j\frac{\sin\omega}{r}\right)\mathrm{d}s_q\\
&\quad + \frac{1}{4\pi}\int_{\Gamma_j}\left((I_{yy}y - I_{yz}z)(2\sin\omega\cos a + (2\ln r - 1)\sin\beta)\right.\\
&\quad \left. - (I_{yy}\cos\beta - I_{yz}\sin\beta)(2\ln r - 1)r\sin\omega\right)\mathrm{d}s_q
\end{aligned} \tag{52b}$$

Moreover, since the torsionless bending problem of beams is solved by the BEM, the domain integrals in Eqs. (3a,b,c), (19), (20), (24a,b,c) and (25) have to be converted to boundary line ones, in order to maintain the pure boundary character of the method. This is accomplished using the Green identity given in Eq. (30) and the Gauss theorem given by the following relations

$$\int_{\Omega_j} g\frac{\partial h}{\partial y}\,\mathrm{d}\Omega_j = -\int_{\Omega_j} h\frac{\partial g}{\partial y}\,\mathrm{d}\Omega_j + \int_{\Gamma_j} hg\cos\beta\,\mathrm{d}s \tag{53a}$$

$$\int_{\Omega_j} g\frac{\partial h}{\partial z}\,\mathrm{d}\Omega_j = -\int_{\Omega_j} h\frac{\partial g}{\partial z}\,\mathrm{d}\Omega_j + \int_{\Gamma_j} hg\sin\beta\,\mathrm{d}s \tag{53b}$$

Thus, using the Gauss theorem for the moments of inertia, the product of inertia and the cross-section area we can write the following relations

$$I_{yy} = \frac{1}{E_1}\sum_{j=1}^{K}\int_{\Gamma_j}\left(E_j - E_i\right)\left(yz^2\cos\beta\right)\mathrm{d}s \tag{54a}$$

$$I_{zz} = \frac{1}{E_1}\sum_{j=1}^{K}\int_{\Gamma_j}\left(E_j - E_i\right)\left(zy^2\sin\beta\right)\mathrm{d}s \tag{54b}$$

$$I_{yz} = \frac{1}{2E_1}\sum_{j=1}^{K}\int_{\Gamma_j}\left(E_j - E_i\right)\left(zy^2\cos\beta\right)\mathrm{d}s \tag{54c}$$

$$A = \frac{1}{2G_1}\sum_{j=1}^{K}\int_{\Gamma_j}\left(G_j - G_i\right)\left(y\cos\beta + z\sin\beta\right)\mathrm{d}s \tag{54d}$$

while the $\{y_S, z_S\}$ coordinates of the shear center S are obtained from the calculation of the following boundary line integrals

$$\begin{aligned} y_S = \frac{1}{4B}\sum_{j=1}^{K}\int_{\Gamma_j}\left(E_j - E_i\right)\Bigg(&\nu I_{zz}\left(\frac{1}{2}y^4 + y^2z^2\right)\cos\beta \\ &+\nu I_{yz}\left(\frac{1}{2}z^4 + y^2z^2\right)\sin\beta - 4(\Phi)_j\left(z\cos\beta - y\sin\beta\right)\Bigg)\mathrm{d}s \end{aligned} \tag{55a}$$

$$\begin{aligned} z_S = \frac{1}{4B}\sum_{j=1}^{K}\int_{\Gamma_j}\left(E_j - E_i\right)\Bigg(&\nu I_{yy}\left(\frac{1}{2}z^4 + y^2z^2\right)\sin\beta + \nu I_{yz}\left(\frac{1}{2}y^4 + y^2z^2\right)\cos\beta \\ &+4(\Theta)_j\left(z\cos\beta - y\sin\beta\right)\Bigg)\mathrm{d}s \end{aligned} \tag{55b}$$

Moreover, applying the Gauss theorem for the functions $\{(\Theta)_j, \partial(\Theta)_j/\partial y\}$, $\{(\Theta)_j, \partial(\Theta)_j/\partial z\}$, $\{(\Phi)_j, \partial(\Phi)_j/\partial y\}$, $\{(\Phi)_j, \partial(\Phi)_j/\partial z\}$, $\{(\Theta)_j, \partial(\Phi)_j/\partial y\}$ and $\{(\Theta)_j, \partial(\Phi)_j/\partial z\}$ the shear deformation coefficients a_y, a_z, $a_{yz} = a_{zy}$ are obtained as

$$a_y = \frac{A}{E_1\Delta^2}\left(\left(4\nu + 2\right)\left(I_{yy}I_{\Theta y} - I_{yz}I_{\Theta z}\right) + \frac{1}{4}\nu^2\left(I_{yy}^2 + I_{yz}^2\right)I_{ed} - I_{\Theta e}\right) \tag{56a}$$

$$a_z = \frac{A}{E_1 \Delta^2}\left((4\nu+2)\left(I_{zz}I_{\Phi z} - I_{yz}I_{\Phi y}\right) + \frac{1}{4}\nu^2\left(I_{zz}^2 + I_{yz}^2\right)I_{ed} - I_{\Phi d}\right) \tag{56b}$$

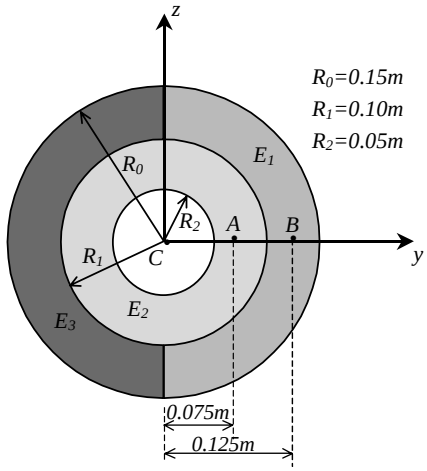

Fig. 2. Composite circular tube cross-section of the cantilever beam of Example 1.

Table 1
Resultant transverse shear stresses at points A and B (kPa) for different Poisson's ratios of the composite circular tube cross-section of Example 1

E_1/E_2	E_3/E_2	$(\tau_\Omega^A)_2$		$(\tau_\Omega^B)_1$	
		Present study	Muskhelishvili (1963)	Present study	Muskhelishvili (1963)
$\nu = 0$					
1	1	8.949181	8.952465	5.514528	5.514719
	2	7.642280	–	4.628520	–
2	2	6.539870	6.542557	5.106785	5.108449
	3	5.946931	–	4.596984	–
3	3	5.136228	5.138963	4.720502	4.722953
	4	4.794630	–	4.375467	–
4	4	4.225295	4.228171	4.435614	4.438568
	5	4.002365	–	4.179056	–
5	5	3.587670	3.590691	4.224006	4.227311
	6	3.430458	–	4.021596	–
$\nu = 0.3$					
1	1	8.260418	8.263814	5.090165	5.090510
	2	7.116921	–	4.306791	–
2	2	6.036552	6.039283	4.713688	4.715491
	3	5.522474	–	4.266888	–
3	3	4.740928	4.743658	4.357084	4.359649
	4	4.445957	–	4.055912	–
4	4	3.900092	3.902927	4.094092	4.097140
	5	3.708003	–	3.870661	–
5	5	3.311531	3.314484	3.898749	3.902133
	6	3.176242	–	3.722733	–

$$a_{yz} = \frac{A}{E_1 \Delta^2}\left((2\nu+2)\left(I_{zz}I_{\Theta z} - I_{yz}I_{\Theta y}\right) + 2\nu\left(I_{yy}I_{\Phi y} - I_{yz}I_{\Phi z}\right) - \frac{1}{4}\nu^2\left(I_{yy}+I_{zz}\right)I_{yz}I_{ed} - I_{\Phi e}\right) \tag{56c}$$

where $I_{\Theta e}$, $I_{\Phi e}$ and $I_{\Phi d}$ are boundary integrals given from

$$I_{\Theta e} = \sum_{j=1}^{K} \int_{\Gamma_j} \left(E_j - E_i\right)(\Theta)_j (\boldsymbol{n}\cdot\boldsymbol{e})\,\mathrm{d}s \tag{57a}$$

$$I_{\Phi e} = \sum_{j=1}^{K} \int_{\Gamma_j} \left(E_j - E_i\right)(\Phi)_j (\boldsymbol{n}\cdot\boldsymbol{e})\,\mathrm{d}s \tag{57b}$$

Table 2
Coordinate of the shear center y_S (cm) with respect to the geometric center of the circles of the composite circular tube cross-section of Example 1

E_1/E_2	E_3/E_2	$\nu = 0$	$\nu = 0.3$
1	2	−2.7997	−2.5323
2	3	−2.0257	−1.8097
3	4	−1.5950	−1.4189
4	5	−1.3174	−1.1696
5	6	−1.1227	−0.9957

Table 3
Shear correction factors for different Poisson's ratios of the composite circular tube cross-section of Example 1

E_1/E_2	E_3/E_2	κ_y	κ_z
$\nu = 0$			
1	1	0.681859 (0.681818) (Cowper, 1966) (0. 681818) (Renton, 1997)	0.681859 (0.681818) (Cowper, 1966) (0. 681818) (Renton, 1997)
	2	0.640786	0.657460
2	2	0.641179	0.641179
	3	0.619113	0.626847
3	3	0.616298	0.616298
	4	0.602910	0.607428
4	4	0.600434	0.600434
	5	0.591500	0.594473
5	5	0.589558	0.589558
	6	0.583187	0.585294
$\nu = 0.3$			
1	1	0.679233 (0.714024) (Cowper, 1966) (0.679188) (Renton, 1997)	0.679233 (0.714024) (Cowper, 1966) (0.679188) (Renton, 1997)
	2	0.638623	0.655198
2	2	0.639397	0.639397
	3	0.617548	0.625189
3	3	0.614919	0.614919
	4	0.601652	0.606107
4	4	0.599284	0.599284
	5	0.590427	0.593355
5	5	0.588554	0.588554
	6	0.582234	0.584310

$$I_{\Phi d} = \sum_{j=1}^{K} \int_{\Gamma_j} \left(E_j - E_i\right)(\Phi)_j (\boldsymbol{n} \cdot \boldsymbol{d})\, \mathrm{d}s \tag{57c}$$

while $I_{\Theta y}$, $I_{\Theta z}$, $I_{\Phi y}$, $I_{\Phi z}$ and I_{ed} are domain integrals given from

$$I_{\Theta y} = \sum_{j=1}^{K} \int_{\Omega_j} E_j (\Theta)_j y \, \mathrm{d}\Omega_j \tag{58a}$$

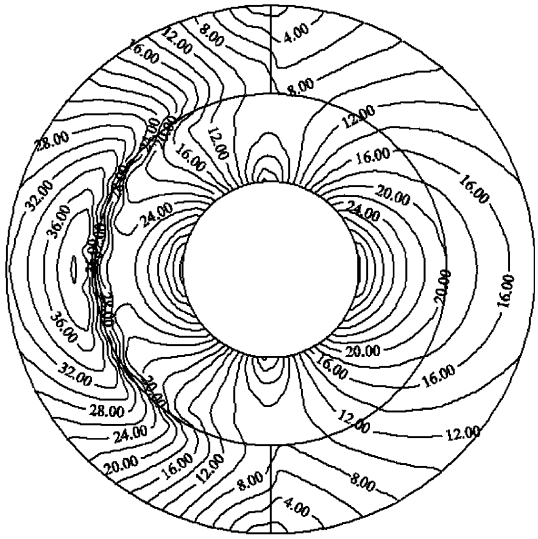

(a) $max\left(\tau_{\Omega}\right)_j = 44.1354kPa$

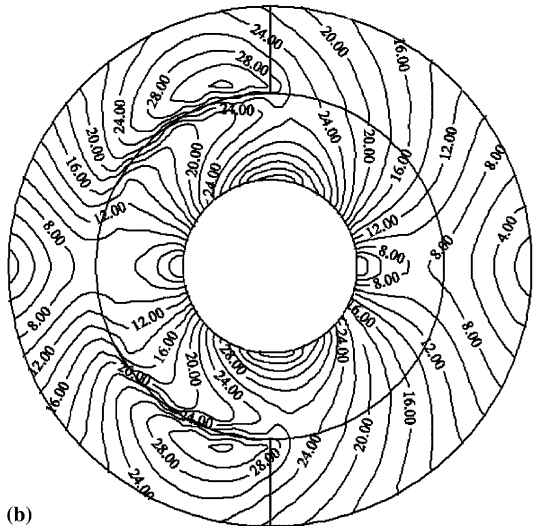

(b)

Fig. 3. Distributions of the resultant transverse shear stress $(\tau_{\Omega})_j$ in the interior of the composite circular tube cross-section of Example 1, for $v = 0.0$, $E_1/E_2 = 1$, $E_3/E_2 = 2$ and for (a) $Q_z = -1$ kN and (b) $Q_y = +1$ kN.

$$I_{\Theta z} = \sum_{j=1}^{K} \int_{\Omega_j} E_j (\Theta)_j z \, \mathrm{d}\Omega_j \tag{58b}$$

$$I_{\Phi y} = \sum_{j=1}^{K} \int_{\Omega_j} E_j (\Phi)_j y \, \mathrm{d}\Omega_j \tag{58c}$$

$$I_{\Phi z} = \sum_{j=1}^{K} \int_{\Omega_j} E_j (\Phi)_j z \, \mathrm{d}\Omega_j \tag{58d}$$

$$I_{ed} = \sum_{j=1}^{K} \int_{\Omega_j} E_j \left(y^4 + z^4 + 2y^2 z^2\right) \mathrm{d}\Omega_j \tag{58e}$$

which can be converted into boundary integrals by applying the Green identity for the functions $\{(\Theta)_j, z^3\}$, $\{(\Theta)_j, y^3\}$, $\{(\Phi)_j, z^3\}$ and $\{(\Phi)_j, y^3\}$ as

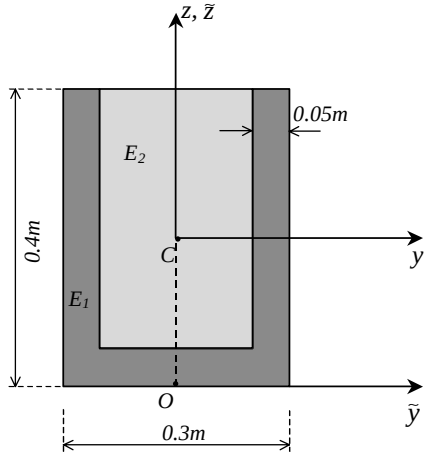

Fig. 4. Composite cross-section of the cantilever beam of Example 2.

Table 4
Coordinate $\tilde{z}_C$ (cm) of the centroid C and resultant transverse shear stress at this point (kPa) for two different cases of concentrated loading and Poisson's ratios of the composite cross-section of Example 2

E_1/E_2	$\tilde{z}_C$	$(\tau_\Omega^C)_2$			
		$Q_z = -1$ kN		$Q_y = +1$ kN	
		$\nu = 0$	$\nu = 0.33$	$\nu = 0$	$\nu = 0.33$
1	20.0	12.498998 (12.5) (EBT)	11.938572	12.499163 (12.5) (EBT)	11.071304
2	18.9706	9.199799	8.728094	10.591865	9.577383
3	18.4091	7.355529	6.953806	9.505636	8.702415
4	18.0556	6.153481	5.804804	8.735040	8.065876
5	17.8125	5.300311	4.992646	8.134598	7.559545
6.837	17.5198	4.235002	3.982239	7.287670	6.829300

$$I_{\Theta y} = \frac{1}{6}\sum_{j=1}^{K}\int_{\Gamma_j}(E_j - E_i)\left[\left(I_{yz}y^3z^2 - 2I_{yy}y^4z\right)\sin\beta + \left(3(\Theta)_j\cos\beta - y(\boldsymbol{n}\cdot\boldsymbol{e})\right)y^2\right]\mathrm{d}s \tag{59a}$$

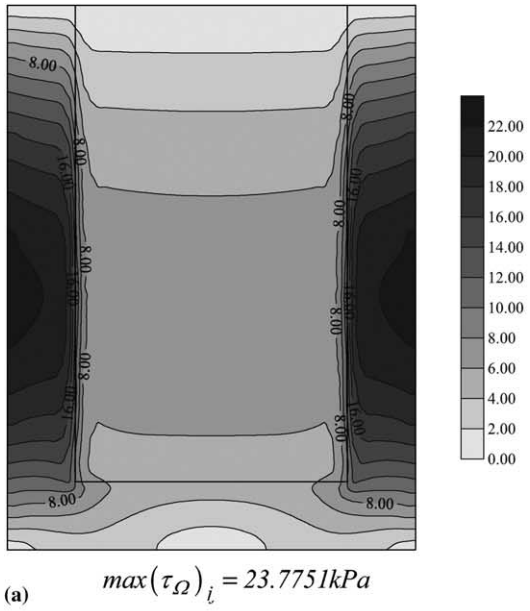

(a) $max(\tau_\Omega)_i = 23.7751kPa$

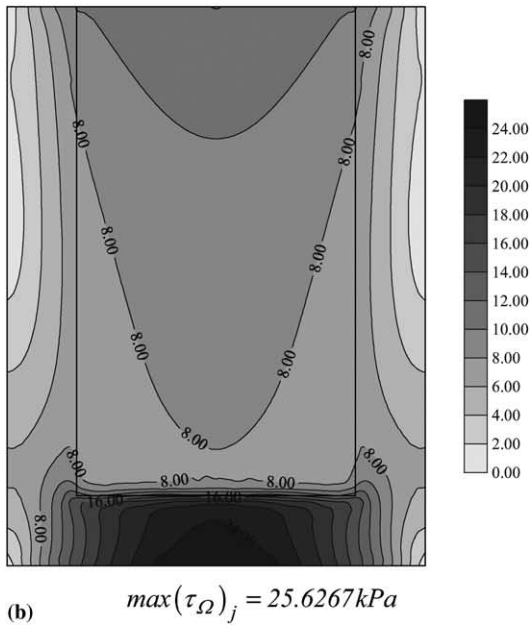

(b) $max(\tau_\Omega)_j = 25.6267kPa$

Fig. 5. Distributions of the resultant transverse shear stress $(\tau_\Omega)_j$ in the interior of the composite cross-section of Example 2, for $v = 0.33$, $E_1/E_2 = 3$ and for (a) $Q_z = -1$ kN and (b) $Q_y = +1$ kN.

Table 5
Coordinate z_S (cm) of the shear center for different Poisson's ratios of the composite cross-section of Example 2

E_1/E_2	$z_S(\equiv z_M)$ for $v = 0$	z_S for $v = 0.33$
1	0.00	0.00
2	−0.5209	−0.4634
3	−1.3516	−1.2773
4	−2.2795	−2.2026
5	−3.2207	−3.1466
6.837	−4.8810	−4.8155
	(−4.89) (Debard, 1997, RDM 5.01 Soft)	
	(−4.90) (Fatmi and Zenzri, 2004)	

Table 6
Shear correction factors for different Poisson's ratios of the composite cross-section of Example 2

E_1/E_2	κ_y		κ_z	
	$v = 0$	$v = 0.33$	$v = 0$	$v = 0.33$
1	0.833427	0.817572	0.833412	0.831403
	(0.833)		(0.833)	
	(SectionBuilder 8.1 Soft)		(SectionBuilder 8.1 Soft)	
2	0.709248	0.701529	0.800961	0.799247
3	0.615573	0.611080	0.776744	0.775299
4	0.547215	0.544287	0.759048	0.757802
5	0.495951	0.493891	0.745721	0.744624
6.837	0.429505	0.428269	0.728338	0.727431
	(0.49442)	(0.428) (Fatmi and Zenzri, 2004)	(0.74757)	(0.727) (Fatmi and Zenzri, 2004)
	(SectionBuilder 8.1 Soft)		(SectionBuilder 8.1 Soft)	
		(0.430)		(0.729)
		(Debard, 1997, RDM 5.01 Soft)		(Debard, 1997, RDM 5.01 Soft)
		(0.40519) (Nouri and Gay, 1994)		(0.70077) (Nouri and Gay, 1994)

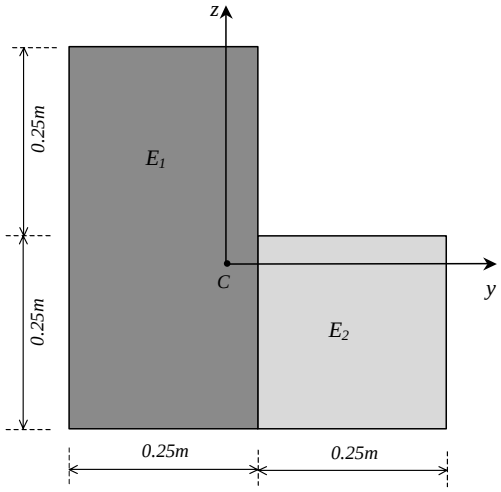

Fig. 6. L-shaped composite cross-section of the cantilever beam of Example 3.

$$I_{\Theta z} = \frac{1}{6}\sum_{j=1}^{K}\int_{\Gamma_j}(E_j - E_i)\left[\left(2I_{yz}z^4 y - I_{yy}z^3y^2\right)\cos\beta + \left(3(\Theta)_j \sin\beta - z(\boldsymbol{n}\cdot\boldsymbol{e})\right)z^2\right]\mathrm{d}s \tag{59b}$$

$$I_{\Phi y} = \frac{1}{6}\sum_{j=1}^{K}\int_{\Gamma_j}(E_j - E_i)\left[\left(2I_{yz}y^4 z - I_{zz}y^3z^2\right)\sin\beta + \left(3(\Phi)_j \cos\beta - y(\boldsymbol{n}\cdot\boldsymbol{d})\right)y^2\right]\mathrm{d}s \tag{59c}$$

$$I_{\Phi z} = \frac{1}{6}\sum_{j=1}^{K}\int_{\Gamma_j}(E_j - E_i)\left[\left(I_{yz}z^3y^2 - 2I_{zz}z^4 y\right)\cos\beta + \left(3(\Phi)_j \sin\beta - z(\boldsymbol{n}\cdot\boldsymbol{d})\right)z^2\right]\mathrm{d}s \tag{59d}$$

$$I_{ed} = \sum_{j=1}^{K}\int_{\Gamma_j}(E_j - E_i)\left(y^4 z\sin\beta + z^4 y\cos\beta + \frac{2}{3}y^2z^3\sin\beta\right)\mathrm{d}s \tag{59e}$$

Finally, using the Gauss theorem the coordinates of the centroid C with respect to the arbitrarily coordinate system $O\tilde{y}\tilde{z}$ are obtained from

$$\tilde{y}_C = \frac{\sum_{j=1}^{K}\int_{\Gamma_j}(E_j - E_i)(\tilde{y}\tilde{z}\sin\beta)\mathrm{d}s}{\frac{1}{2}\sum_{j=1}^{K}\int_{\Gamma_j}(E_j - E_i)(\tilde{y}\cos\beta + \tilde{z}\sin\beta)\,\mathrm{d}s}, \quad \tilde{z}_C = \frac{\sum_{j=1}^{K}\int_{\Gamma_j}(E_j - E_i)(\tilde{y}\tilde{z}\cos\beta)\mathrm{d}s}{\frac{1}{2}\sum_{j=1}^{K}\int_{\Gamma_j}(E_j - E_i)(\tilde{y}\cos\beta + \tilde{z}\sin\beta)\mathrm{d}s} \tag{60a, b}$$

4. Numerical examples

On the basis of the analytical and numerical procedures presented in the previous sections, a computer program has been written and representative examples have been studied to demonstrate the efficiency, the accuracy and the range of applications of the developed method.

Example 1. A cantilever beam of the composite circular tube cross-section shown in Fig. 2 has been studied. In Table 1 the resultant transverse shear stresses $(\tau_{\Omega}^{A})_2$, $(\tau_{\Omega}^{B})_1$ at points A and B of the cross-section of the beam loaded at its free end by a concentrated force $Q_y = +1$ kN and for the Poisson's ratios $v = 0$, $v = 0.3$ are presented as compared wherever possible with those obtained from an analytical solution

Table 7
Distance d_{CS} and maximum resultant transverse shear stress $\tau_{\max}$ for various Poisson's ratios of the composite cross-section of Example 3, subjected to the concentrated load $Q = \sqrt{Q_z^2 + Q_y^2}$, with $Q_z = -1$ kN and $Q_y = +1$ kN

E_1/E_2	d_{CS} (cm)		$\tau_{\max}$ (kPa)	
	$v = 0$	$v = 0.3$	$v = 0$	$v = 0.3$
1	6.59556 (6.575) (Sauer, 1980)	6.70703	53.2551	53.1197
2	6.02817	6.15889	39.9117	39.9311
3	5.60475	5.75888	33.7153	33.7357
4	5.21824	5.37945	30.0376	30.0580
5	4.86748	5.02780	27.5426	27.5702
6	4.55255	4.70848	25.7086	25.7480
7	4.27094	4.42106	24.2885	24.3419
8	4.01912	4.16294	23.1485	23.2165
9	3.79340	3.93092	22.2089	22.2915
10	3.59042	3.72184	21.4187	21.5154

(Muskhelishvili, 1963). The accuracy of the obtained results is remarkable. Also, the resulting discrepancy of the values of the shear stresses, arising from the different values of the Poisson's ratio v leads to the conclusion that the influence of this material constant cannot be ignored. Moreover, in Tables 2 and 3 the shear center coordinate y_S with respect to the geometric center of the circles and the shear correction factors κ_y, κ_z (values in parentheses come from Cowper's (1966) definition and from an analytical formula developed by Renton (1997)) for various values of the Poisson's ratio are presented, respectively. The alteration of the shear center coordinate with the Poisson's ratio variation is noteworthy. We remind here the coincidence of the shear center and the center of twist, in the case of $v = 0$. Finally, in Fig. 3 the distributions of the interior resultant shear stress $(\tau_\Omega)_j$ $(j = 1, 2, 3)$ for two different cases of concentrated loading are presented.

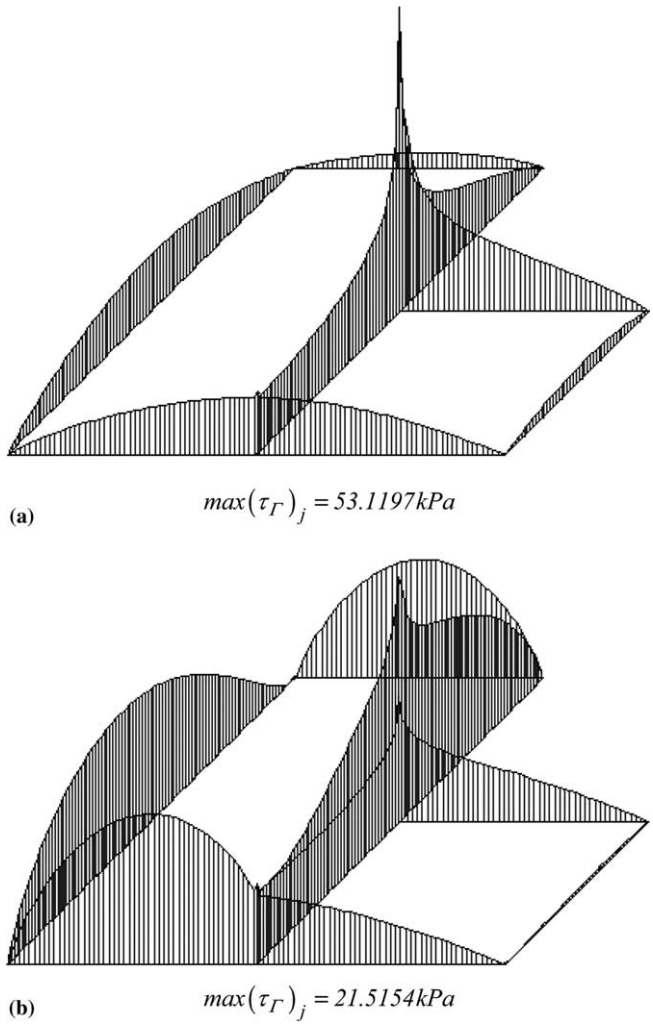

Fig. 7. Distributions of the resultant transverse shear stress $(\tau_\Gamma)_j$ along the boundary of the composite cross-section of Example 3, subjected to the concentrated load $Q = \sqrt{Q_z^2 + Q_y^2}$, with $Q_z = -1$ kN and $Q_y = +1$ kN, for $v = 0.3$ and for (a) $E_1/E_2 = 1$ and (b) $E_1/E_2 = 10$.

Example 2. A cantilever beam having the cross-section shown in Fig. 4 has been studied. In Table 4 the coordinate $\tilde{z}_C$ of the centroid C with respect to the arbitrary coordinate system $O\tilde{y}\tilde{z}$ and the resultant transverse shear stress $(\tau_Q^C)_2$ at this point (values in parentheses come from engineering beam theory (EBT) (Timoshenko and Goodier, 1984)), for the Poisson's ratios $v = 0$, $v = 0.33$ and for two different cases of

Table 8
Shear correction factors κ_y, κ_z and κ_{yz} of the composite cross-section of Example 3, for various Poisson's ratios

E_1/E_2	$v = 0$			$v = 0.3$		
	κ_y	κ_z	κ_{yz}	κ_y	κ_z	κ_{yz}
1	0.69480 (0.69809) (Nastran 4.0 Soft)	0.69480 (0.69809) (Nastran 4.0 Soft)	−9.39352	0.68901	0.68901	−10.4203
2	0.63197	0.74809	−9.96204	0.62603	0.74391	−10.8879
3	0.58882	0.76979	−9.47095	0.58254	0.76650	−10.2073
4	0.56314	0.78161	−9.13537	0.55641	0.77889	−9.75711
5	0.54800	0.78912	−8.97955	0.54077	0.78680	−9.53309
6	0.53932	0.79439	−8.95006	0.53155	0.79235	−9.46158
7	0.53475	0.79833	−9.00643	0.52643	0.79651	−9.49145
8	0.53288	0.80141	−9.12245	0.52401	0.79977	−9.59073
9	0.53285	0.80391	−9.28115	0.52341	0.80240	−9.73916
10	0.53408	0.80599	−9.47129	0.52408	0.80460	−9.92353

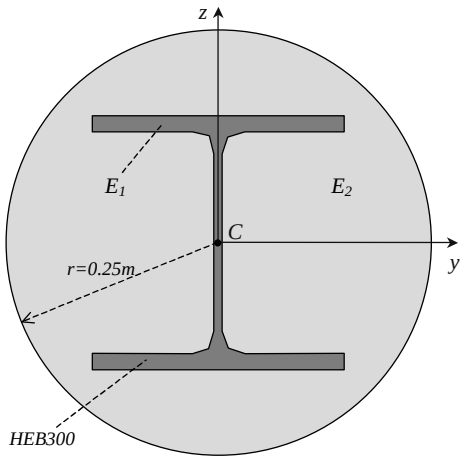

Fig. 8. Composite cross-section of the cantilever beam of Example 4.

Table 9
Maximum resultant transverse shear stress τ_{max} for various load cases and for Poisson's ratio $v = 0.3$, of the composite cross-section of Example 4

E_1/E_2	τ_{max} (kPa)		
	Q_z	Q_y	Q
5	33.8033	28.4209	37.3976
6	39.9672	32.5527	43.5241
7	45.9167	36.3060	49.2961
8	51.6564	39.7361	54.7514
9	57.1926	42.8877	59.9221
10	62.5327	45.7976	64.8351

concentrated loading are presented. The influence of the Poisson's ratio v is once more verified. Moreover, in Fig. 5 the distributions of the interior resultant shear stress $(\tau_\Omega)_j$ $(j = 1, 2, 3)$ for two different cases of concentrated loading are presented. Finally, in Tables 5 and 6 the shear center coordinate z_S with respect to the centroid C of the composite cross-section and the shear correction factors κ_y, κ_z for the Poisson's ratios $v = 0$ and $v = 0.33$ are presented, respectively, as compared wherever possible with those obtained from 2-D FEM solutions (Debard, 1997–RDM 5.01 Soft, SectionBuilder 8.1 Soft, Nouri and Gay, 1994) and from a 3-D FEM solution (Fatmi and Zenzri, 2004) of the 'exact' elastic beam theory (Ladevéze and Simmonds, 1998). Both the accuracy of the results (in Tables 5 and 6) between BEM and 3-D FEM solutions and the discrepancy of the results (in Table 6) between BEM and 2-D FEM (SectionBuilder 8.1 Soft), arisen from the ignorance of boundary conditions at the interfaces, are easily verified. Noting both Table 3 of the first example and Table 6 of this example, the minor alteration of the shear correction factors with the Poisson's ratio variation is also verified.

Example 3. A cantilever beam having the L-shaped composite cross-section shown in Fig. 6 has been studied. In Table 7 the distance d_{CS} between centroid C and shear center S of the composite cross-section and the maximum resultant transverse shear stress $\tau_{\max}$ for the concentrated load $Q = \sqrt{Q_z^2 + Q_y^2}$, with $Q_z = -1$ kN and $Q_y = +1$ kN for various Poisson's ratios are presented, as compared wherever possible with those obtained from another BEM solution (Sauer, 1980). Moreover, in Fig. 7 for the same loading the boundary distributions of the resultant transverse shear stress $(\tau_\Gamma)_j$ for various E_1/E_2 ratios and in Table 8 the shear correction factors κ_y, κ_z and κ_{yz} for various Poisson's ratios of the composite cross-section are presented, as compared wherever possible with those obtained from a 2-D FEM solution (Nastran 4.0 Soft). The minor alteration of both the shear deformation coefficients and the shear center coordinate with the Poisson's ratio variation are noteworthy.

Table 10
Shear correction factors κ_y, κ_z for Poisson's ratio $v = 0.3$ of the composite cross-section of Example 4

E_1/E_2	κ_y	κ_z
5	0.838187	0.708029
6	0.830843	0.677910
7	0.823672	0.650976
8	0.816794	0.626828
9	0.810262	0.605101
10	0.804093	0.585472

Table 11
Shear correction factors κ_y, κ_z for various homogeneous steel HEB cross-sections ($v = 0.3$)

HEB	κ_y			κ_z		
	BEM	TTT	Error (%)	BEM	TTT	Error (%)
300	0.6876	0.7647	−11.2129	0.2166	0.3181	−46.8606
400	0.6488	0.7281	−12.2226	0.2656	0.3538	−33.2078
500	0.6220	0.7040	−13.1833	0.2961	0.3764	−27.1192
600	0.5864	0.6668	−13.7108	0.3354	0.4105	−22.3912
700	0.5487	0.6267	−14.2154	0.3771	0.4475	−18.6688
800	0.5197	0.5925	−14.0081	0.4080	0.4840	−18.6275
900	0.4907	0.5656	−15.2639	0.4360	0.5084	−16.6055
1000	0.4626	0.5399	−16.7099	0.4613	0.5312	−15.1528

Example 4. A cantilever beam having the composite cross-section consisting of a HEB-300 (Eurocode No 3) totally encased in a circular matrix, as shown in Fig. 8, has been studied. In Table 9 the maximum resultant transverse shear stress $\tau_{\max}$ of the composite cross-section subjected to various load cases ($Q_z = -1$ kN, $Q_y = +1$ kN and $Q = \sqrt{Q_z^2 + Q_y^2}$) and in Table 10 the shear correction factors κ_y, κ_z are presented, for various E_1/E_2 ratios. Moreover, in order to determine the discrepancy due to the assumption of constant transverse shear stress along the thickness coordinate followed by the 'refined models', in Table 11 the shear correction factors κ_y, κ_z of the special case of various homogeneous steel HEB cross-sections are presented as compared with those obtained from the thin tube theory (TTT), in which the aforementioned assumption is followed (Vlasov, 1961). As expected the accuracy of the results of the thin tube theory (TTT) is increased with the decrement of the thickness of the cross-section members (flanges' thickness increases and web's thickness decreases with the increment of the HEB code). Finally, in Fig. 9 the boundary distributions of the resultant transverse shear stress $(\tau_\Gamma)_j$ for two load cases are presented.

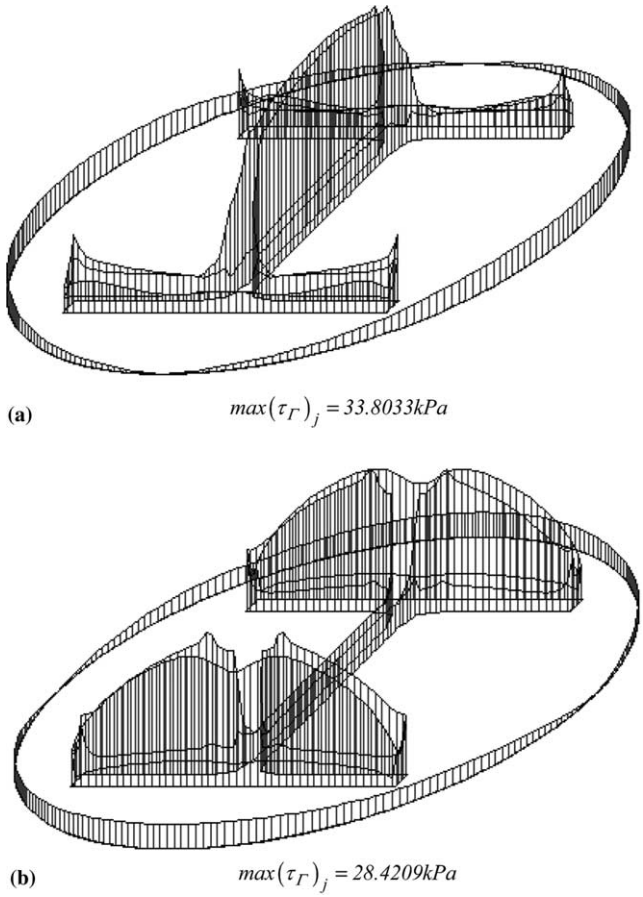

Fig. 9. Distributions of the resultant transverse shear stress $(\tau_\Gamma)_j$ along the boundary of the composite cross-section of Example 4, for (a) $Q_z = -1$ kN and (b) $Q_y = +1$ kN, for Poisson's ratios $\nu = 0.3$ and $E_1/E_2 = 5$.

5. Concluding remarks

In this paper a boundary element method is developed for the solution of the general transverse shear loading problem of beams of arbitrary composite constant cross-section. Two boundary value problems that take into account the effect of Poisson's ratio are formulated with respect to stress functions and solved employing a pure BEM approach. The evaluation of the transverse shear stresses at any interior point is accomplished by direct differentiation of these stress functions, while both the coordinates of the shear center and the shear deformation coefficients are obtained from these functions using only boundary integration. The main conclusions that can be drawn from this investigation are

(a) The numerical technique presented in this investigation is well suited for computer aided analysis for beams of arbitrary composite cross-section, while the analysis is performed with respect to an arbitrary system of axes and not necessarily the principal one.
(b) The convergence of the obtained results employing the proposed numerical procedure with those obtained from a 3-D FEM solution applied to the 'exact' elastic beam theory is easily verified.
(c) The resulting discrepancy of the shear stresses, arising from different values of the Poisson's ratio v demonstrates the significant influence of this material constant.
(d) Engineering beam theory can give accurate results only in homogeneous cross-sections with continuous variation of width and zero Poisson's ratio.
(e) The alteration of the shear center coordinates and the shear deformation coefficients with the Poisson's ratio variation is not significant.
(f) Ignorance of the continuity conditions of transverse shear stresses at interfaces leads to discrepancies in the results.
(g) The assumption that the transverse shear stress along the thickness coordinate remains constant is right only in thin-walled cross-sections.
(h) The accuracy of the results is remarkable.
(i) The developed procedure retains the advantages of a BEM solution over a pure domain discretization method since it requires only boundary discretization.

Acknowledgments

Financial support for this work provided by the "*Iraklitos Research Fellowships with Priority to Basic Research*", an EU funded project in the special managing authority of the Operational Program in Education and Initial Vocational Training.

References

Chou, S.I., 1993. Determination of centers of flexure using the boundary element method. Engineering Analysis with Boundary Elements 12, 321–324.

Cowper, G.R., 1966. The shear coefficient in Timoshenko's Beam theory. Journal of Applied Mechanics, ASME 33 (2), 335–340.

Debard, Y., 1997. Logiciel de calcul des structures par la méthode des éléments finis. Version RDM5.01. Institut Universitaire de Technologie, Le Mans, France.

Eurocode No 3, 1993. Design of steel structures, Part 1–1: General rules and rules for Buildings, European Committee for Standardization (CEN), ENV 1993-1-1/April 1992.

Fatmi, R.E., Zenzri, H., 2004. Numerical method for the exact elastic beam theory. Applications to homogeneous and composite beams. International Journal of Solids and Structures 41, 2521–2537.

Friedman, Z., Kosmatka, J.B., 2000. Torsion and flexure of a prismatic isotropic beam using the boundary element method. Computers and Structures 74, 479–494.

Goodier, J.N., 1944. A theorem on the shearing stress in beams with applications to multicellular sections. Journal of Aeronautical Sciences 11, 272–280.

Gruttmann, F., Wagner, W., 2001. Shear correction factors in Timoshenko's beam theory for arbitrary shaped cross-sections. Computational Mechanics 27, 199–207.

Gruttmann, F., Wagner, W., Sauer, R., 1998. Zur Berechnung der Schubspannungen aus Querkräften in Querschnitten Prismatisher Stäbe mit der Methode der Finiten Elemente. Bauingenieur 73 (11), 485–490.

Gruttmann, F., Sauer, R., Wagner, W., 1999. Shear stresses in prismatic beams with arbitrary cross-sections. International Journal for Numerical Methods in Engineering 45, 865–889.

Hutchinson, J.R., 2001. Shear coefficients for Timoshenko beam theory. ASME Journal of Applied Mechanics 68, 87–92.

Karama, M., Afaq, K.S., Mistou, S., 2003. Mechanical behavior of laminated composite beam by the new multi-layered laminated composite structures model with transverse shear stress continuity. International Journal of Solids and Structures 40 (6), 1525–1546.

Koczyk, S., 1994. Wölbkrafttorsion und Querkraftschubspannungen in einem Balken bei FE—Diskretisierung seines Querschnitts. Technische Mechanik, Wissenschaftliche Zeitschrift für Anwendungen der Technischen Mechanik, Universität Magdeburg 14 (1), 3–13.

Ladevéze, P., Simmonds, J.G., 1998. New concepts for linear beam theory with arbitrary geometry and loading. European Journal of Mechanics, A/Solids 17 (3), 377–402.

Love, A.E.H., 1952. A Treatise on the Mathematical Theory of Elasticity. Dover Publications, New York.

Mason, W.E., Herrmann, L.R., 1968. Elastic shear analysis of general prismatic beams. Journal of Engineering Mechanics Division, ASCE 94 (EM4), 965–983.

MSC/NASTRAN for Windows, 1999. Finite element modeling and postprocessing system. Help System Index,Version 4.0, USA.

Muskhelishvili, N.I., 1963. Some Basic Problems of the Mathematical Theory of Elasticity. P. Noordhoff Ltd.

Nouri, T., Gay, D., 1994. Shear stresses in orthotropic composite beams. International Journal of Engineering Science 32, 1647–1667.

Osgood, W.R., 1943. The Centre of Shear again. Journal of Applied Mechanics 10 (2), A-62–A-64.

Pilkey, W.D., 2002. Analysis and Design of Elastic Beams—Computational Methods. Wiley, New York.

Reddy, J.N., 1989. On refined computational models of composite laminates. International Journal for Numerical Methods in Engineering 27, 361–382.

Reissner, E., Tsai, W.T., 1972. On the determination of the centers of twist and of shear for cylindrical shell beams. Journal of Applied Mechanics 39, 1098–1102.

Renton, J.D., 1997. A note on the form of the shear coefficient. International Journal of Solids and Structures 34, 1681–1685.

Sapountzakis, E.J., 2000. Solution of nonuniform torsion of bars by an integral equation method. Computers and Structures 77, 659–667.

Sauer, E., 1980. Schub und Torsion bei Elastischen Prismatischen Balken, Mitteilungen aus dem Institut für Massivbau der Technischen Hochschule Darmstadt, vol. 29, Verlag Wilhelm Ernst & Sohn, Berlin/München.

Schramm, U., Kitis, L., Kang, W., Pilkey, W.D., 1994. On the shear deformation coefficient in beam theory. Finite Elements in Analysis and Design 16, 141–162.

Schramm, U., Rubenchik, V., Pilkey, W.D., 1997. Beam stiffness matrix based on the elasticity equations. International Journal for Numerical Methods in Engineering 40, 211–232.

SectionBuilder, 2002. Section Builder and Designer for Concrete, Steel and Composite Sections. User's Manual and Technical Reference, Version 8.1, Computer and Structures, Inc., Berkeley, California, USA.

Sokolnikoff, I.S., 1956. Mathematical Theory of Elasticity. McGraw-Hill, New York.

Stephen, N.G., 1980. Timoshenko's shear coefficient from a beam subjected to gravity loading. ASME Journal of Applied Mechanics 47, 121–127.

Timoshenko, S.P., Goodier, J.N., 1984. Theory of Elasticity, third ed. McGraw-Hill, New York.

Touratier, M., 1992a. A generalization of shear deformation theories for axisymmetric multi-layered shells. International Journal of Solids and Structures 29 (11), 1379–1399.

Touratier, M., 1992b. A refined theory of laminated shallow shells. International Journal of Solids and Structures 29 (11), 1401–1415.

Trefftz, E., 1935. Über den Schubmittelpunkt in einem durch eine Einzellast gebogenen Balken. ZAMM 15, 220–225.

Vlasov, V.Z., 1961. Thin Walled Elastic Beams. English Translation, National Science Foundation, Washington, DC, U.S. Dept. Commerce.

Weber, C., 1924. Biegung und Schub in Geraden Balken. ZAMM 4, 334–348.

Weinstein, A., 1947. The centre of shear and the centre of twist. Quarterly of Applied Mathematics 5 (1), 97–99.